Jour. Fac. Sci., Hokkaido Univ., Ser. IV,
vol. 23, no. 2 Aug., 1992, pp. 227-245

DIATOMACEOUS SEDIMENTS ALONG THE PACIFIC COASTAL AREAS OF SOUTH AMERICA AND THEIR EVALUATION

by

Itaru Koizumi

(with 3 text-figures, 4 tables and 2 plates)

Abstract

The Tertiary diatomaceous sediments in the sequences along the continental margin from Ecuador to Chile are recognized in 4 horizons at the last stage of transgression-regression cycle. (1) The uppermost Eocene Chira Formation in Bayovar of northern Peru was resulted from high-latitude cooling and consequently strengthened oceanic circulation, the Terminal Eocene Event. (2) The Caballas Formation in Cerro Las Salinas of Pisco consists of calcareous siltstone and sandstone with interbedded diatomaceous intervals. It is assigned to the late Oligocene to early Miocene based on diatom biostratigraphy. The diatom assemblages contain many tropic to equatorial species. (3) The significant diatomaceous sediments in Ecuador, Peru, and Chile occur in early middle Miocene at 14 to 12 Ma. They were triggered by intensified coastal upwelling and oceanic circulation from pole to equatorial zone caused by the increased thermal gradients resulted from the permanent establishment of the major East Antarctic ice sheet. Sedimentary facies changes simultaneously both in the Pacific coastal area of South America and in the North Pacific region. (4) The upper Miocene to Pliocene diatomaceous sediments such as Pisco Formation in Pisco-Ice of Peru contain abundantly coastal upwelling-related genus *Thalassionema* and *Chaetoceros*, and suggest high productivity conditions linked to coastal upwelling. Tertiary diatomaceous sediments along the Pacific coastal areas of South America are related to the global climatic and oceanic events.

Introduction

The biostratigraphic researches based on planktonic microfossils have made it possible to correlate some local geologic events with others over the world. Paleoclimatic and paleoceanographic changes in the Neogene, common scales to correlate events, are based on the distribution of deep-sea hiata, fluctuations on $\delta^{18}O$ of foraminiferal tests, distribution of sea-floor sediments, and changes of biogeographic conditions. All of them are gained from analyzing the drilled cores by the Deep Sea Drilling Project and the Ocean Drilling Program.

Fluctuations on $\delta^{18}O$ of benthic foraminifera in the west equatorial Pacific region (Woodruff *et al.*, 1981; Miller *et al.*, 1987; Williams, 1988) indicate that in the end of Eocene to early Oligocene the major continental ice sheet established and rapidly enlarged 36-35 Ma. Ice sheet presumably enlarged again 31 Ma, 25 Ma, 14.5-14 Ma, and even 10-8 Ma, but significant cooling began 14 Ma when East Antarc-

Contribution from the Department of Geology and Mineralogy, Faculty of Science, Hokkaido University, No. 2068

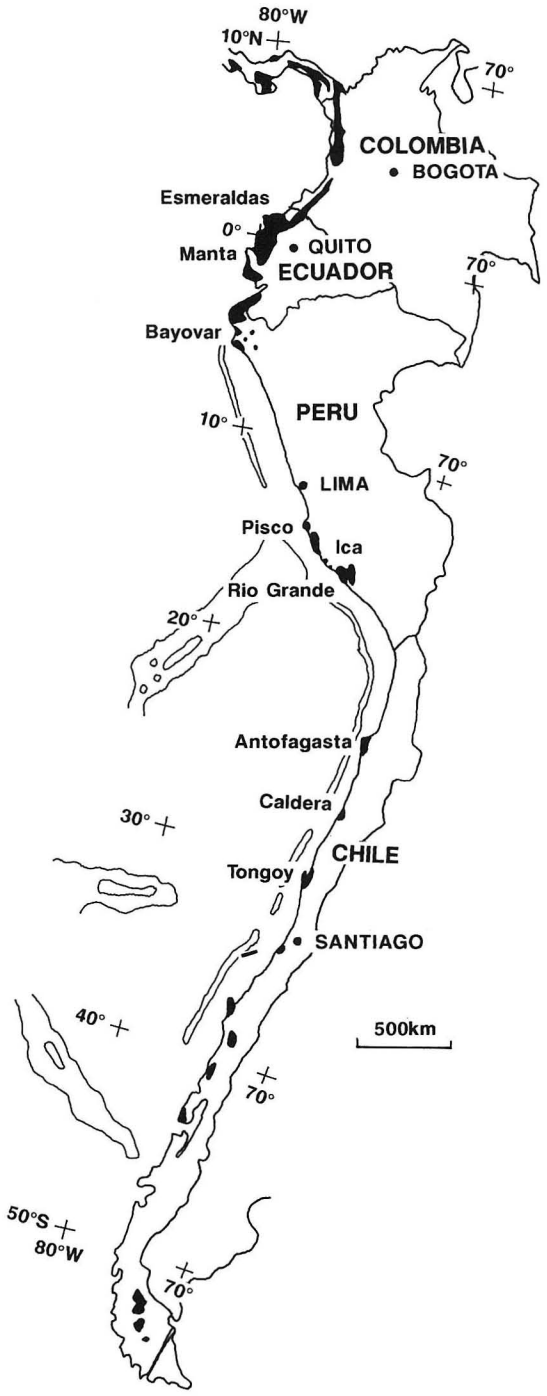

Text-fig. 1 Distribution of marine Cenozoic strata on the Pacific coastal area of South America.

tic ice sheet reached the coast. The whole earth was cooled by the ice sheet that enlarged and diminished alternately since then.

Bio-siliceous sediments began to deposit in the east Equatorial Pacific (Keller and Barron, 1983), California (Barron, 1986), and Japan (Koizumi, 1986a, 1990b) since 18 Ma, but they occur abruptly over the wide area in the marginal North-Pacific (Ingle, 1981; Koizumi, 1986b) at 16.0-15.5 Ma. The sediments contain the diatom assemblages composed mainly of warm-water species (Barron, 1986; Barron and Baldauf, 1990; Koizumi, 1990b). The component species of the diatom assemblages and the frequency of them show that diatomaceous sediments in the middle Miocene (13.3-9.0 Ma) were formed under intensified bottom-water circulation and upwelling due to climatic cooling; the cooling caused disappearance, by 13.5 Ma, of tropic to subtropic species which flourished since early Miocene and caused insteadly appearance of mid-high latitudes species, present oceanic circulation and present distribution of sea-floor sediments.

The Pacific coastal side of the South America is one of the major coastal upwelling areas in the world oceans. The upwelling offshore of Ecuador, Peru, and northern Chile is caused by the combination of pole-equator Peru (Humbold) Current and southeast Trade Wind. As the Coriolis force turns the surface water to the west, cold subsurface water wells up. The upwelling water is undersaturated in oxygen but rich in nutrients such as phosphates and nitrates. Sedimentary sequences associated with coastal upwelling contain diatomaceous, organic-rich siltstone and shales, organic dolomites, and phosphorites. The diatomaceous sediments formed by this coastal upwelling have not yet been analyzed nor correlated, while those sediments in the North America or Japan area have already given lots of informations.

The purpose of this paper is to present the biostratigraphic data and paleoceanographic environment of the Tertiary diatomaceous sediments along the Pacific coastal areas of the South America by means of diatoms.

Materials and Methods

Tertiary diatom assemblages have been quantitatively examined in land-sections along the coastal side of Ecuador, Peru, and Chile (Text-fig. 1). Locations, route-map, lithostratigraphy, and fossil occurrences of mollusca, planktonic foraminifera, and calcareous nannoplankton in selected sections are summarized in Tsuchi (1988, 1990).

Original material was treated by hydrogen peroxide and hydrochloric acid. Pleurax was used as a mounting medium. All diatoms were identified and counted up to 100-200 individuals in each count at 1250 x. Neogene diatom biostratigraphy in the low-latitude of the eastern Pacific Ocean has been studied by Burckle (1972, 1978) and Barron (1983, 1985), but the study has not yet extended into the mid-latitude. And the zonation can not easily apply to the Tertiary sediments on the Pacific coastal sections of the South America, because ocurrences of zonal marker

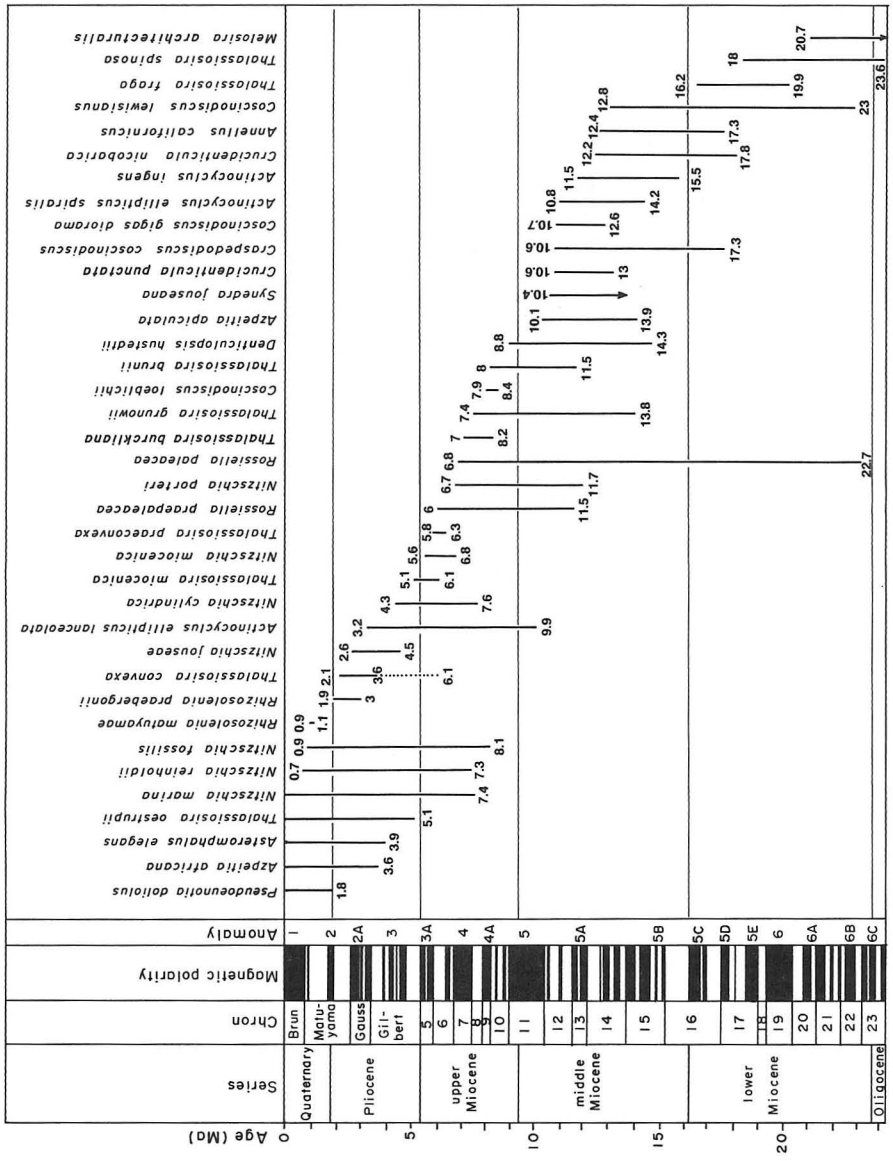

Text-fig. 2 Ranges of stratigraphically useful diatoms in the Cenozoic of low latitudes applied to the age determination of Cenozoic strata on the Pacific coastal area of South America [compiled Burckle (1972, 1978) and Barron (1983, 1985)]. The paleomagnetic scale is from Berggren *et al.* (1985).

species, all of which are oceanic planktonic species, are very rare through these sections. Age-determinations by means of diatoms are, therefore, given now in absolute age (Ma) on the basis of ranges of stratigraphically useful species (Text-fig. 2). Paleogene planktonic diatom zonation, especially Eocene to Oligocene, in the lower latitude has been presented by Fenner (1984), and Kim and Barron (1986).

Results

Ecuador

The lower part of the Viche Formation (Samples Ec-24 and Ec-23) along Rio Esmeraldas in Esmeraldas, contains *Thalassiosira fraga* as well as *Cestodiscus pulchellus*, *Coscinodiscus lewisianus*, *Raphidodiscus marylandicus*, and *Synedra jouseana*, and is age-assigned consequently to 17.4-16.7 Ma (Table 1). The upper part of the Viche Formation (Ec-22) produces *Crucidenticula punctata, Denticulopsis hustedtii,* and *Thalassiosira grunowii*, and can be age-assigned to 13.7-12.1 Ma. Samples Ec-13 and Ec-14, belong to the lower part of the Onzole Formation, contain *Cr. punctata, D. hustedtii, Hemidiscus cuneiformis*, and *Thalassiosira flexosa*, which is age-assigned to 12.5-12.1 Ma. Sample Ec-12 belonging to the uppermost part of the Onzole Formation is presumed to be 1.8-0.65 Ma, because of the presence of *Nitzschia fossilis*, *Pseudoeunotia doliolus, Thalassiosira oestrupii,* and *H. cuneiformis*, but coexisting planktonic foraminifera indicate N. 21 and calcareous nannoplankton NN18. Therefore, the first appearance of *P. doliolus* is presumed to be older than 1.8 Ma in the Ecuador.

Ec-5 and Ec-6, sampled from the Onzole Formation in San Vicente, north of Manta, contain *S. jouseana* and *T. fraga* with planktonic foraminifera indicating N. 5-N. 6 and calcareous nannoplankton indicating NN2-NN3. Additionaly, Ec-6 contains *Craspedodiscus coscinodiscus, R. marylandicus*, and *S. jouseana*, and is age-assigned to 17.3-16.7 Ma, but planktonic foraminiferal assemblages within it indicate N. 4-N. 6. Samples Ec-5 and Ec-6 coincide at the uppermost range of age-assignment. Samples Ec-8 and Ec-9, from the Villingota Member of the upper Tosagua Formation contain *H. cuneiformis, T. flexosa*, and *Thalassiosira brunii*, and is age-assigned to 12.5-8.6 Ma. This coincides with NN8-NN10 which calcareous nannoplankton assemblages indicate, but does not with N. 16-N. 18 planktonic foraminifera indicate.

Ec-11 from the Tosagua Formation in Jaramijo, east of Manta, contains *Actinocyclus ingens* which coincides with N. 8-N. 10 of planktonic foraminifera and NN5 of calcareous nannoplankton.

Peru

Sample Pe-1, taken from the Chira Formation which distributes along the coast in Bayovar, southwest of Piura, contains such index species of the upper Eocene, as *Cymatosira coronata, Pyxilla gracilis*, and *Triceratium barbadense* as well

Table 1 Occurrence of diatom taxa in Ecuador.

Formation	Viche			Onzole					Tosagua					
Samples									8		9		11	
Species	24	23	22	13	14	12	6	5	1	2	1	4	1	2
Actinocyclus ellipticus				+					+		+	+		
A. ingens													+	+
Actinoptychus senarius		+		+		+	+	+	+	+	+	+		
Azpeitia endoi	+	+	+											
A. nodulifer						+					+	+		
A. tabularis						+								
A. vetustissima		+												
Cestodiscus pulchellus	+	+												
C. sp.							+							
Coscinodiscus lewissianus	+						+							
C. marginatus		+	+	+		+		+	+					+
C. nitidus						+								
C. rhombicus		+												
Craspedodiscus coscinodiscus							+							
Crucidenticula punctata			+	+										
Denticulopsis dimorpha						+								
D. hustedtii			+	+										
D. praekatayamae			+											
Hemidiscus cuneiformis				+		+					+	+		
Nitzschia fossilis						+								
N. jouseae						+								
N. miocenica											+			
Paralia sulcata			+	+		+			+	+	+			
Pseudoeunotia doliolus						+								
Raphidodiscus marylandica	+	+					+							
Rhizosolenia alata									+					
R. bergonii						+								
R. miocenica									+		+			
R. styliformis				+					+		+			
Stephanopyxis turris									+	+				
Synedra jouseana	+	+					+	+						
Thalassionema nitzschioides			+	+		+		+	+		+	+		
Thalassiosira antiqua												+		
T. brunii										+		+		
T. eccentrica						+					+			
T. flexosa			+	+							+			
T. fraga	+	+					+							
T. grunowii			+	+		+								
T. leptopus				+		+					+			
T. oestrupii						+								
Thalassiothrix longissima	+		+	+			+							

Table 2 Occurrence of the Paleogene diatom taxa in Peru. Caba=Caballas.

Formation	Chira		Caba	
Samples	1		88-7	
Species	1	5	7	5
Actinocyclus octonarius	2			
Actinoptychus senarius	10	7		
Asteromphalus hiltonianus	1			
Cestodiscus antarcticus				+
C. reticulatus				+
Coscinodiscus marginatus	2			
C. mutabilis				+
C. oculus-iridis		2		
C. praenitida			+	+
C. rhombicus			+	
C. sp.	31	9		
Cymatosira compacta		5		
C. coronata		+		
C. fossilis		4		
Eucampia balaustium		2		
Hemiaulus ambiguus		1		
H. dubius				+
H. kittonii		1		+
H. orthoceras				+
H. polycystinorum				+
H. pungens				+
H. weissflogii		2		
H. spp.	11	16		
Lithodesmium sp.	3	1		
Melosira architecturalis		+		+
M. areolata				+
Paralia sulcata	2	1	+	
Pseudodimerogramma elegans				+
Pyxilla gracilis		+	+	
Raphidodiscus marylandicus			+	
Rhaphoneis amphiceros		4		
R. gemmifera	4			
Rhizosolenia alata		3		
R. calcar avis		2		
R. habetata	3	12		
Stellarima sp.				+
Stephanopyxis ferox	1			
S. turris	8	13	+	
S. spp.	15	5		
Synedra jouseana				+
Triceratium arcticum	1			
T. barbadense	+			
T. macroporum			+	
T. reticulum	2	4		
T. schulzii		1		

Table 3 Occurrence of the Neogene diatom taxa in Peru. LB=Las Burias.

Formation	Zapallar				Pisco				LB
Samples	8	9	7		16	14			88 9 2
Species	2	2	1	4	1	1	5	9	
Actinocyclus curvatulus			1	3	4			1	
A. ellipticus					1				
A. octonarius	2	1		3			2	1	
A. octonarius var. tenellus				3				+	
Actinoptychus senarius	6	16		3	15			1	+
A. splendens					3				
Azpeitia nodulifer				7	2		1		
A. vetustissima	+								+
Coscinodiscus marginatus			6	2	1				+
C. oculus-iridis				2			1		
C. perforatus		+		+	2		+		+
C. radiatus					1				
C. symbolophorus							+		
Delphineis angustata							55	1	+
D. ischaboensis	2	2							
Denticulopsis hustedtii	+	2		+	1				+
D. praedimorpha				+					
Eucampia sp.					6				
Grammatophora marina				+					+
Hemidiscus cuneiformis				+					
Lithodesmium minusculum									+
L. undulatum	2				2				
Medialia splendida									+
Nitzschia cylindrica	+			+					
N. cfr. extincta								3	+
N. fossilis				+		+			
N. jouseae							+		
N. miocenica		+				+			
N. porteri		+		+					
Odontella aurita							2	10	+
O. sinensis								8	
Paralia sulcata				1					
Pseudoeunotia doliolus								+	
Rhizosolenia hebetata				6					
R. styliformis	1				2				+
Rossiella paleacea	+								
Rouxia californica	1				2				
R. moholensis		1							+
R. naviculiodes	2	9							
Stephanopyxis turris	2	5		1	2			1	+
Synedra indica	12	3		5	7				+
S. jouseana					1				+
Thalassionema nitzschioides	32	20	4	35	45	+	37	70	+
Thalassiosira antiqua				1					
T. brunii	3	+							+
T. eccentrica				8					
T. flexosa	4	2			+				+
T. leptopus	1						+	+	
T. pacifica				1				2	
T. plicatoides	4	+							
T. subtilis				3					
T. sp. A	24	33					1	2	
T. sp. B	2	1					1		
Thalassiothrix longissima	2			1	2				+

as *Melosira atchitecturalis* and *Triceratium schulzii* (Table 2). Pe-3-3, from the Tablazo Formation which overlaps the Chira Formation unconformably, contains species which is characteristic in coastal upwelling area such as *Actinoptychus senarius, Paralia sulcata, Skeletonema costatum,* and *Cymatosira* sp. with many resting spores of a genus *Chaetoceros* as well. Planktonic foraminifera indicates N. 22.

Samples Pe-8 and Pe-9, from the Zapallar Formation in Pampa Los Hornillos, south of Piura, contain *Nitzschia porteri, Rossiella paleacea, Rouxia californica, T. brunii, D. hustedtii,* and *T. flexosa*, and are presumed to be 9.8-8.8 Ma (Table 3). Pe-6 and Pe-7 from the Zapallar Formation in La Mina contain *Nitzschia cylindrica, N. porteri,* and *N. fossilis*, which give them age-assignment to 7.6-6.7 Ma.

Samples Pe-86-17 and Pe-88, from the Caballas Formation in Cerro Las Salinas, south of Pisco, contain species that indicate the upper Oligocene to the lower Miocene such as *Coscinodiscus rhombicus, M. architecturalis, Ra. marylandicus,* and *S. jouseana,* as well as *Hemiaulus kittonii, Hemiaulus polycystinorum, Hemiaulus pungens, Coscinodiscus praenitida,* and *Triceratium macroporum* (Table 2).

Pe-16 sampled from the Pisco Formation in Cerro Lechuza, south of Pisco, contains *D. hustedtii, R. californica,* and *T. flexosa,* and is age-assigned to 13.9-8.8 Ma (Table 3).

The Pisco Formation (Pe-14) in Rio Pisco, northeast of Pisco, contains in the lower part *Nitzschia miocenica* and *N. fossilis* which are age-assigned to 7.3-5.6 Ma, in the middle part *N. jouseae* which is age-assigned to 4.5-2.6 Ma, and in the upper part *P. doliolus,* 2.0-0 Ma. Consequently, the Pisco Formation is age-assigned to 7.3-0 Ma in the maximum range.

The lower part of the Las Burias Formation (Pe-88-0-2) in Rio Grande, southwest of Palpa, contains *D. hustedtii, S. jouseana,* and *T. flexosa*, and is age-assigned to 13.9-10.4 Ma.

Chile

The middle-upper part of the Mejillones Formation (Ch-88-3-12), located along the coast of Caleta Herradura de Mejillones north of Antofagasta, contains *A. ingens, C. lewisianus, Cr. nicobarica, D. hustedtii,* and *S. jouseana,* and is age-assigned to 13.9-12.8 Ma (Table 4). This age coincides with an age of N. 9-N. 10 that coexisting planktonic foraminifera indicate. The diatomite in the uppermost part of this formation (Ch-86-3-21—Ch-86-3-18) is assigned to the uppermost Miocene-lower Pliocene (6.0-2.5 Ma) (Koizumi, 1990a). The diatomite (Ch-5 and Ch-6) in Cuenca del Tibron, north of Antofagasta, contains, *N. jouseae, N. reinholdii, T. convexa,* and *T. oestrupii,* and is age-assigned to 4.5-2.6 Ma, which is coincident with N. 21 that coexisting planktonic foraminiferal assemblage indicates.

The diatomite (Ch-10 — Ch-12) in Quebrada Blanca, east of Caldera and Ch-15 in Bahia Inglesa, south of Caldera, contains *N. fossilis, N. jouseae,* and *T. oestrupii*, and is age-assigned also 4.5-2.6 Ma. This age is coincident with N. 21 that

Table 4 Occurrence of diatom taxa in Chile. M=Mejillones, Ingle.=Inglesa.

Formation	M.	Tibron			Quebrada Blanca					Ingle.		El Rincon		
Samples	88 3 12	6 3	5 1	5 10	11 2	10 2	10 5	12 1	12 2	15 1	15 4	19 1	88-1 1	88-1 3
Actinocyclus curvatulus				5	2	+	3			1	6			
A. ellipticus				+										
A. ingens	11													
A. octonarius	9	1		2	26					4	5	1		
Actinoptychus senarius	11	38	12	16	12	13	22	7	3	14	31			
A. splendens								3	2	1				
Anaulus birostratus					1	1		1		1				
Azpeitia nodulifer		18	98			+	6				3	2	+	
A. tabularis	2													
A. vetustissima				4										
Coscinodiscus elegans	2													
C. lewissianus	4													
C. marginatus	9										1			
C. nitidus	2	1			+						+			
C. oculus-iridis				+		1		1						
C. perforatus						1			1					
C. stellaris	+													
Craspedodiscus coscinodiscus	1													
Crucidenticula nicobarica	1													
C. punctata	1													
Delphineis angustata	2													
D. ischaboensis					1									
D. surirella			1		4	4	14	8		6	8			
Denticulopsis hustedtii	20												+	+
D. praekatayamae												18	+	
Grammatophora spp.	6	4	10	3	+	3	7	6	6	3	3	+		
Hemidiscus cuneiformis						1	16			3	3			
Nitzschia fossilis					+	1	5	1				+		
N. jouseae		+				+	13				9			
N. marina		+		1							3			
N. reinholdii				1			1				14	1		
N. spp.					6	14								
Odontella aurita					99	2	4	5		6	10	2		
Paralia sulcata		6	54				4	19	18	16	2			
Rhaphoneis amphiceros								4	2		1			
Rhizosolenia alata		14				7	13							
R. barboi				1						+				
R. hebetata											3			
R. miocenica														+
R. setigera		1				1	1							
R. styliformis		21	6	15	1	1	2	2		18	2			
Rossiella paleacea	1													
Rouxia diploneides												5		
R. naviculoides												7	+	+
Stephanopyxis turris	4			81				1						
S. schenckii												+		+
Synedra jouseana	3			1								4	+	
Thalassionema nitzschioides	56	47	2	19	6	55	50	13		99	74	99	+	
Thalassiosira convexa		5												
T. ecccentrica		18	1	20	3		2	1			2	7		
T. ferelineata		4	1		9	1								
T. flexosa	2											1	+	+
T. jacksonii							1							
T. leptopus							3	2			1			
T. lineata		2		3	2	1						1		
T. oestrupii		2		4	1		1	1			5			
T. pacifica		8		8	1						2			
T. temperei														+
Thalassiothrix longissima	33		3	6		4		2		1		3		

planktonic foraminiferal assemblage in the sample Ch-10 indicates.

Samples Ch-19 and Ch-88-11 from the El Rincon Formation in Tongoy Beach contains *D. hustedtii, S. jouseana, T. flexosa,* and *Stephanopyxis schenckii* together, and are age-assigned to 13.7-10.4 Ma. Coexisiting planktonic foraminiferal assemblages indicate a little younger N. 8b-N. 9.

Conclusions

Neogene diatomaceous sediments in Pacific coastal area along Ecuador to Chile appear frequently in the major four horizons (Text-fig. 3).

(1) The upper Eocene diatomaceous sediments are the oldest in this area, which suggest that cold upwelling existed as early as 40-36 Ma B. P. Cooling in the high-latitude region and consequent intensification of ocean circulation is presumed to have caused this sedimentation.

(2) The uppermost Oligocene to lowest Miocene diatomaceous sediments is intercalated in calcareous siltstone to sandstone, and consist of equatorial and tropical diatom species. $\delta^{18}O$ in this period indicates warm climate over the earth with no ice sheet in the high-latitude region.

(3) In Ecuador, Peru, and Chile, diatomaceous sediments significatly appear at the beginning of the middle Miocene (14-20 Ma B. P.), and contain middle-latitudinal warm and cold diatom species. A series of drilled cores of ODP Leg 112, off-shore Peru, shows that continuous occurrence of diatomaceous sediments began 14 Ma B. P. (Suess, von Huene, *et al.*, 1988). Establishing of East Antarctic ice sheet is presumed to have caused development of bottom currents and following intensification of upwelling.

(4) The upper Miocene to Pliocene diatomaceous sediments contain much of the genus *Chaetoceros* and genus *Thalassionema*, specific in coastal upwelling diatoms.

These diatomaceous sediments are presumed to be at the last stage of transgressiom-regression cycle that begin with coarse-grained sediments abutted upon basement rocks (Dunbar *et al.*, 1990). This sequential sedimentation resembles the strata of organic diatomaceous sediments which occur in circum North Pacific regions. There is, presumably, a close relationship between development of the strata in different locations and worldwide effect of some climatic and oceanic events.

Acknowledgements

This study was made under the Monbusho International Scientific Program of Japan No. 62043033 " Trans-Pacific Correlation of Cenozoic Geohistory " (1985-1987) and No. 63041065 " Trans-Pacific Correlation of Neogene Geologic Events " (1988-1989). I thank Professor Emeritus Ryuichi Tsuchi of the Shizuoka University for giving me an opportunity of participating in field-works. Special thanks are due to my wife Mineko for helping me in re-reading and correcting my English.

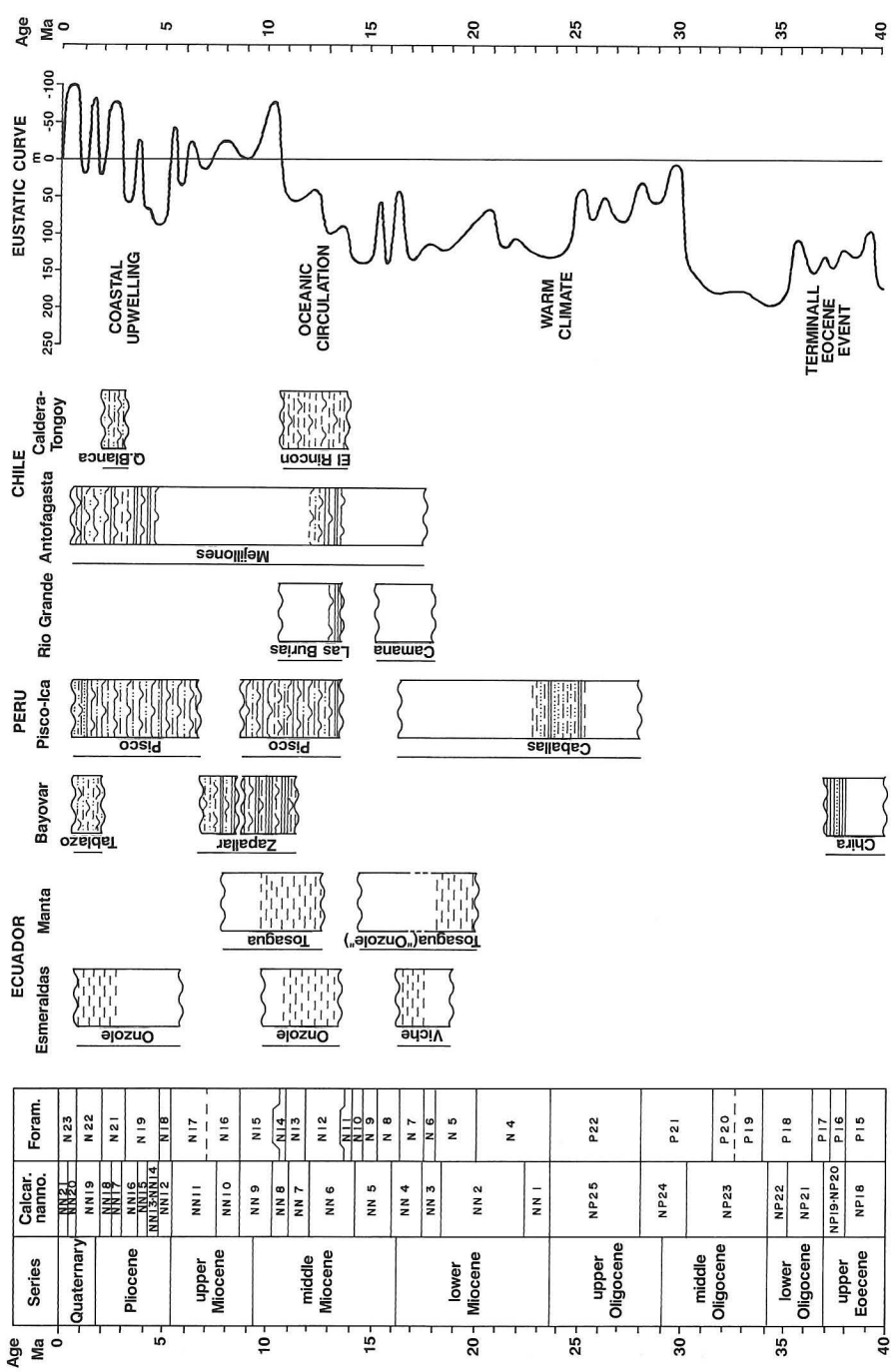

Text-fig. 3 Biostratigraphic correlation chart based on diatom stratigraphy and paleoceanographic events in comparison to the eustatic curve (Haq *et al.*, 1987). Age assignment of the microfossil zones after Haq *et al.* (1987).

Floral references

Actinocyclus curvatulus Janisch
Actinocyclus ellipticus Grunow
Actinocyclus ellipticus f. *lanceolata* Kolbe
Actinocyclus ellipticus var. *spiralis* Barron
Actinocyclus ingens Rattray
Actinocyclus octonarius Ehrenberg
Actinocyclus octonarius var. *tenellus* (Brébisson) Hendey
Actinoptychus senarius Ehrenberg
Actinoptychus splendens (Shadbolt) Ralfs
Anaulus birostratus (Grunow) Grunow
Annellus californicus Tempère
Asteromphalus elegans Greville
Asteromphalus hiltonianus (Greville) Ralfs
Azpeitia africana (Janisch) G. Fryxell and T. P. Waykins
Azpeitia apiculata Sims
Azpeitia endoi (Kanaya) P. A. Sims and G. Fryxell
Azpeitia nodulifer (Schmidt) G. Fryxell and P. A. Sims
Azpeitia tabularis (Grunow) G. Fryxell and P. A. Sims
Azpeitia vetustissima (Pantocsek) P. A. Sims
Cestodiscus antarcticus Fenner
Cestodiscus pulchellus Greville
Cestodiscus reticulatus Fenner
Coscinodiscus elegans Greville
Coscinodiscus gigas var. *diorama* (Schmidt) Grunow
Coscinodiscus lewisianus Greville
Coscinodiscus loeblichii Barron
Coscinodiscus marginatus Ehrenberg
Coscinodiscus mutabilis Strelnikova
Coscinodiscus nitidus Gregory
Coscinodiscus oculus-iridis Ehrenberg
Coscinodiscus perforatus Ehrenberg
Coscinodiscus praenitida Fenner
Coscinodiscus radiatus Ehrenberg
Coscinodiscus rhombicus Castracane
Coscinodiscus stellaris Roper
Coscinodiscus symbolophorus Grunow
Craspedodiscus coscinodiscus Ehrenberg
Crucidenticula nicobarica (Grunow) Akiba and Yanagisawa
Crucidenticula punctata (Schrader) Akiba and Yanagisawa
Cymatosira compacta Schrader and Fenner
Cymatosira coronata Fenner and Schrader
Cymatosira fosslils Schrader
Delphineis angustata (Pantocsek) Andrews
Delphineis ischaboensis (Grunow) Koizumi
Delphineis surirella (Ehrenberg) Andrews
Denticulopsis dimorpha (Schrader) Simonsen
Denticulopsis hustedtii (Kanaya and Simonsen) Simonsen
Denticulopsis praekatayamae Yanagisawa and Akiba
Denticulopsis praedimorpha (Akiba) Barron
Eucampia balaustium Castracane
Grammatophora marina (Lyngbye) Kützing
Hemiaulus ambiguus Grunow
Hemiaulus dubius Grunow
Hemiaulus kittonii Grunow

Hemiaulus orthoceras Strelnikova
Hemiaulus polycystinorum Ehrenberg
Hemiaulus pungens Grunow
Hemiaulus weissflogii Pantocsek
Hemidiscus cuneiformis Wallich
Lithodesmium minusculum Grunow
Lithodesmium undulatum Ehrenberg
Mediaria splendida Sheshukova-Poretzkaya
Melosira architecturalis Brun
Melosira areolata Moissejewa
Nitzschia cylindrica Burckle
Nitzschia extincta Kozurenko and Sheshukova-Poretzkaya
Nitzschia fossilis (Frenguelli) Kanaya and Koizumi
Nitzschia jouseae Burckle
Nitzschia marina Grunow
Nitzschia miocenica Burckle
Nitzschia porteri Frenguelli sensu Burckle
Nitzschia reinholdii Kanaya and Koizumi
Odontella aurita Agardh
Odontella sinensis (Greville) Grunow
Paralia sulcata (Ehrenberg) Cleve
Pseudodimerogramma elegans Schrader
Pseudoeunotia doliolus (Wallich) Grunow
Pyxilla gracilis Tempêre and Forti
Raphidodiscus marylandicus Christian
Rhaphoneis amphiceros Ehrenberg
Rhaphoneis gemmifera Ehrenberg
Rhizosolenia alata Brightwell
Rhizosolenia barboi Brun
Rhizosolenia bergonii Peragallo
Rhizosolenia calcar vis M. Schultze
Rhizosolenia hebetata (Bailey) Gran
Rhizosolenia styliformis Brightwell
Rhizosolenia matuyamai Burckle
Rhizosolenia miocenica Schrader
Rhizosolenia praebergonii Mukhina

Explanation of Plate 1
Magnifications are x1500.

Fig. 1 *Melosira architecturalis* Brun, Sample Pe-1-1 in the Chira Formation, Peru.
Fig. 2 *Triceratium barbadense* Greville, Sample Pe-1-1 in the Chira Formation, Peru.
Fig. 3 *Thalassiosira fraga* Schrader, Sample Ec-6 in the Onzole Formation, Ecuador.
Fig. 4 *Thalassiosira flexosa* (Brun) Akiba and Yanagisawa, Sample Ec 9-1 in the Tosagua Formation, Ecuador.
Fig. 5 *Cymatosira coronata* Fenner and Schrader, Sample Pe-1-5 in the Chira Formation, Peru.
Fig. 6 *Thalassiosira oestrupii* (Ostenfeld) Proshkina-Lavrenko, Sample Ch-12-1 in the diatomite in Quebrada Blanca. Chile.
Fig. 7 *Thalassiosira brunii* Akiba and Yanagisawa, Sample Ec-9-4 in the Tosagua Formation, Ecuador.
Fig. 8 *Thelassiosira convexa* Muchina, Sample Ch-6-3 in the diatomite in Cuenca del Tibron, Chile.
Fig. 9 *Hemiaulus kittonii* Grunow, Sample Pe-1-5 in the Chira Formation, Peru.
Fig. 10 *Azpeitia endoi* (Kanaya) P. A. Sims and G. Fryxell, Sample Ec-22 in the Viche Formation, Ecuador.
Fig. 11 *Triceratium schulzii* Jousê, Sample Pe-1-5 in the Chira Formation, Peru.

Plate 1

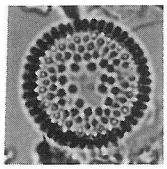

1

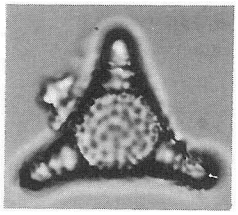

2

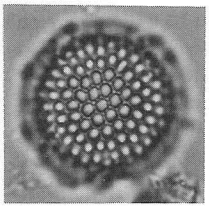

3a

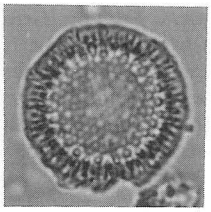

3b

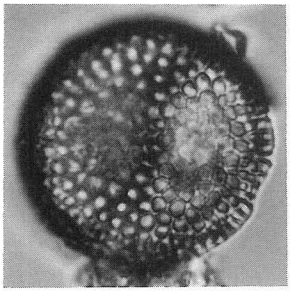

4

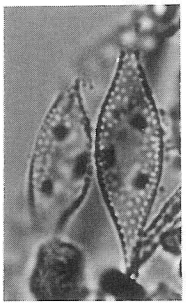

5

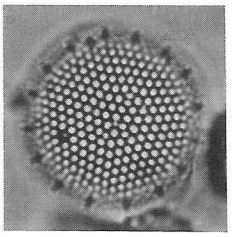

6

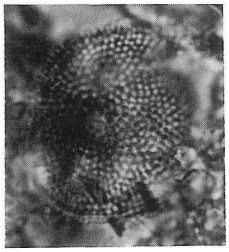

7

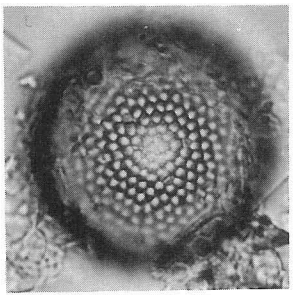

8a

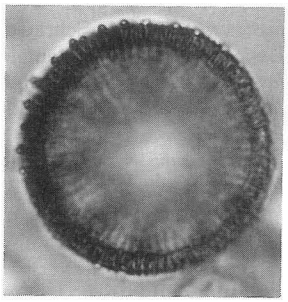

8b

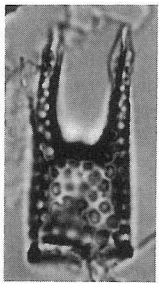

9

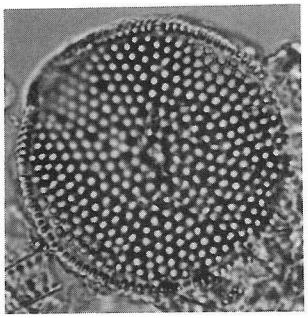

10

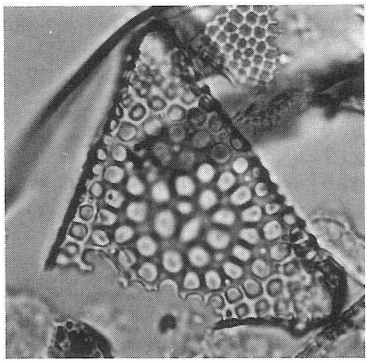

11

Rhizosolenia setigera Brightwell
Rhizosolenia styliformis Brightwell
Rossiella paleacea (Grunow) Desikachary and Maheshwari
Rossiella praepaleacea (Schrader) Gersonde and Schrader
Rouxia californica Peragallo
Rouxia diploneides Schrader
Rouxia naviculoides Schrader
Rouxia moholensis Schrader
Skeletonema costaum (Greville) Cleve
Stephanopyxis ferox (Greville) Ralfs
Stephanopyxis schenckii Kanaya
Stephanopyxis turris (Greville and Arnott) Ralf
Synedra indica Taylor
Synedra jouseana Scheschukova-Poretzkaya
Thalassionema nitzschioides Grunow
Thalassiosira antiqua (Grunow) Cleve-Euler
Thalassiosira brunii Akiba and Yanagisawa
Thalassiosira burckliana Schrader
Thalassiosira convexa Mukhina
Thalassiosira eccentrica (Ehrenberg) Cleve
Thalassiosira ferelineata Hasle and G. Fryxell
Thalassiosira flexosa (Brun) Akiba and Yanagisawa
Thalassiosira fraga Schrader
Thalassiosira grunowii Akiba and Yanagisawa
Thalassiosira jacksonii Koizumi and Barron
Thalassiosira leptopus (Grunow) Hasle and Fryxell
Thalassiosira lineata Jousé
Thalassiosira miocenica Schrader
Thalassiosira oestrupii (Ostenfeld) Proshkina-Lavrenko
Thalassiosira pacifica Gran and Angst
Thalassiosira praeconvexa Burckle
Thalassiosira spinosa Schrader
Thalassiosira subtilis (Ostenfeld) Gran
Thalassiosira temperei (Brun) Akiba and Yanagisawa
Thalassiothrix longissima (Cleve) Cleve and Grunow

Explanation of Plate 2
Magnifications are x1500.

Fig. 1 *Denticulopsis hustedtii* (Simonsen and Kanaya) Simonsen, Sample Ec-10-3 in the Onzole Formation, Ecuador.
Fig. 2 *Nitzschia jouseae* Burckle, Sample Ch-15-4 in the diatomite in Bahia Inglesa, Chile.
Fig. 3 *Nitzschia miocenica* Burckle, Sample Pe-15-9 in the Pisco Formation, Peru.
Fig. 4 *Nitzschia porteri* Frenguelli, Sample Pe-9-2 in the Zapallar Formatiom, Peru.
Fig. 5 *Nitzschia cylindrica* Burckle, Sample Pe-7-4 in the Zapallar Formation, Peru.
Fig. 6 *Nitzschia fossilis* (Frenguelli) Kanaya, Sample Pe-15-9 in the Pisco Formatiom, Peru.
Fig. 7 *Pyxilla gracilis* Tempere and Forti, Sample Pe-1-1 in the Chira Formation, Peru.
Fig. 8 *Nitzschia reinholdii* Kanaya, Sample Ch-15-4 in the Pisco Formation, Peru.
Fig. 9 *Rossiella paleacea* (Grunow) Desikachary and Maheshwari, Sample Pe-8-2 in the Zapallar Formation, Peru.
Fig. 10 *Rouxia californica* M. Peragallo, Sample Pe-8-2 in the Zapallar Formation, Peru.
Fig. 11 *Hemiaulus polycystinorum* Ehrenberg, Sample Pe-1-5 in the Chira Formation, Peru.
Fig. 12 *Coscinodiscus lewisianus* Greville, Sample Ec-6 in the Onzole Formation, Ecuador.
Fig. 13 *Hemidiscus cuneiformis* Wallich, Sample Ch-10-5 in the diatomite in Quebrada Blanca, Chile.
Fig. 14 *Hemiaulus weissflogii* Pantocsek, Sample Pe-1-5 in the Chira Fomation, Peru.

Plate 2

1

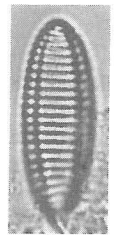

2

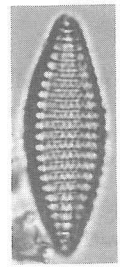

3

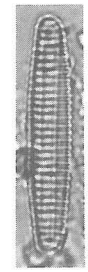

4

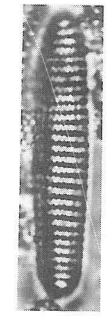

5

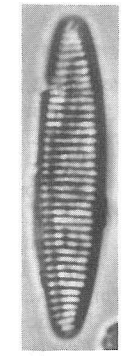

6

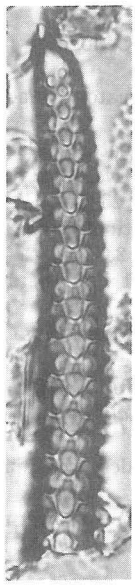

7

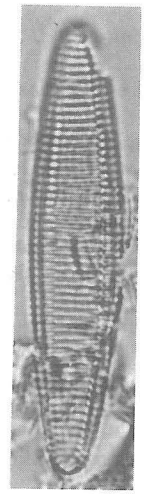

8

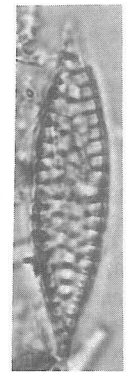

9

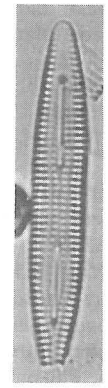

10

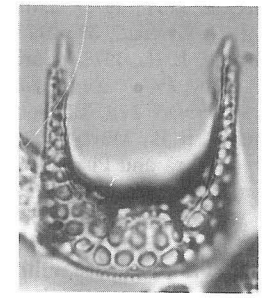

11

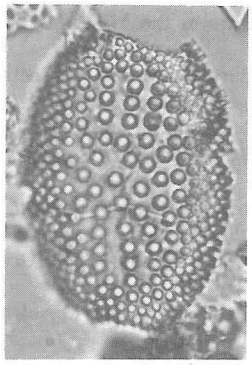

12

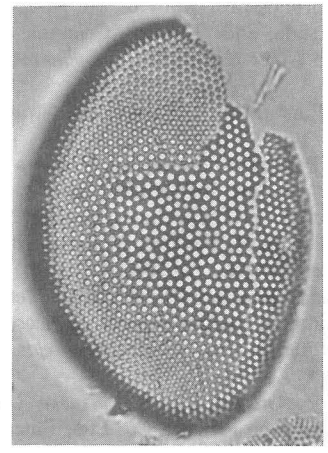

13

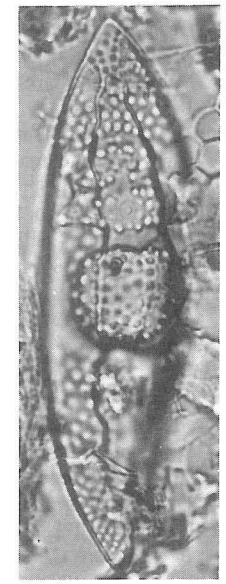

14

Triceratium schulzii Jousé

References

Barron, J. A., 1983. Latest Oligocene through early middle Miocene diatom biostratigraphy of the eastern tropical Pacific. *Mar. Micropaleontol.*, 7 : 487-515.

Barron, J. A., 1985. Late Eocene to Holocene diatom biostratigraphy of the equatorial Pacific Ocean, DSDP Leg 85. In : Mayer, F., Theyer, F., et al. (eds.), *Init. Repts. DSDP*, 85, Washington, D. C., U. S. . Govt. Printing Office. pp. 413-456.

Barron, J. A., 1986. Response of equatorial Pacific diatoms to polar cooling during the middle Miocene. In : Ricard, M. (ed.), *Proc. 8th Init. Diatom Symp.*, Paris, August 27—September 1, 1984. Koeltz, W. Germany, pp. 591-600.

Barron, J. A., and Baldauf, J. G., 1990. Development of biosiliceous sedimentation in the North Pacific during the Miocene and early Pliocene. In : Tsuchi, R. (ed.), *Pacific Neogene Events-Their Timing, Nature and Interrelationship-*. University of Tokyo Press, Tokyo, pp. 43-63.

Berggren, W. A., Kent, D. V., Flynn, J. J., and van Couvering, J. A., 1985. Cenozoic geochronology. *Geol. Soc. Amer. Bull.*, 96 : 1407-1418.

Burckle, L. H., 1972. Late Cenozoic planktonic diatom zoned from the eastern equatorial Pacific. *Nova Hed.*, 39 : 217-246.

Burckle, L. H., 1978. Early Miocene to Pliocene diatom datum levels for the equatorial Pacific. In : *Proc. 2nd Working Group Meet., Biostratigr. Datum-Planes Pacific Neogene, IGCP Project 114*, Bandung, 1977, Spec. Publ. Geol. Res. Dev. Cent. Indones., 1 : 25-44.

Dunber, R. B., Marty, R. C., and Baker, P. A., 1991. Cenozoic marine sedimentation in the Sechura and Pisco basins, Peru. *Palaeogeogr., Palaeoclimatol., Palaeoecol.*, 77 : 235-261.

Fenner, J., 1984. Eocene-Oligocene planktonic diatom stratigraphy in high and low latitudes. *Micropaleontology*, 30 : 319-342.

Haq, B. U., Hardenbol, J., and Vail, P. R., 1987. Chronology of fiuctuating sea levels since the Traiassic (250 million years ago to present). Science, 235 : 1158-1167.

Ingle, J. C., 1981. Origin of Neogene diatomites around the North Pacific Rim. In : Garrison, R. E., et al. (eds.), *The Montery Formation and Related Siliceous Rocks of California*. Spec. Publ. Pac. Ser., Soc. Econ. Paleontol. Mineral., pp. 159-179.

Keller, G., and Barron, J. A., 1983. Paleoceanographic implications of Miocene deep-sea hiatus. *Geol. Soc. Amer., Bull.*, 94 : 590-613.

Kim, W. H., and Barron, J. A., 1986. Diatom biostratigraphy of the upper Oligocene to lowermosr Miocene San Gregorio Formation. Baja California Sur, Mexico. *Diatom Research*, 1 : 169-187.

Koizumi, I., 1986a. Diatom biochronostratigraphy of the Neogene in the Joban coal-field, Northeast Japan-Yunagaya, Shirado, and Takaku Groups-. In : Nakagawa, H., et al. (eds.), *Essays in Geology-Professor Nobu Kitamura Commemorative Volume-*. Tokou Printing Co. Ltd., Sendai, pp. 175-191.

Koizumi, I., 1986b. Siliceous sedimentation and paleoceanographic events in the Miocene. *Mar. Sci. Mon.*, 18 : 46-53.

Koizumi, I., 1990a. Miocene to Pliocene diatoms from Caleta Herradura de Mejillones section, Chile. In : Tsuchi, R. (ed.), *Reports of Anden Studies, Shizuoka University-Trans-Pacific Correlation of Cenozoic Geohistory-*. Kurofune Printing Co. Ltd., Shizuoka, 3 : 17-22.

Koizumi, I., 1990b. Successional changes of middle Miocene diatom assemblages in the northwest Pacific. *Palaeogeogr., Palaeoclimatol., Palaeoecol.*, 77 : 181-193.

Miller, K. G., Fairbanks, R. G., and Mountain, G. S., 1987. Tertiary oxygen isotope syntheses, sea level history, and continental margin erosion. *Paleoceanography*, 2 : 1-19.

Suess, E., von Huene, R., et al., 1988. *Proc. ODP, Init. Repts.*, 12 : College Station, TX (Ocean Drilling Program) : 1-1015.

Tsuchi, R. (ed.), 1988. *Reports of Andean Studies, Shizuoka University-Trans-Pacific Correlation of Cenozoic Geohistory.* Kurofune Printing Co. Ltd., Shizuoka, 2 : 1-108.

Tsuchi, R. (ed.), 1990. *Reports of Andean Studies, Shizuoka University-Trans-Pacific Correlation*

of Cenozoic Geohistory. Kurofune Printing Co. Ltd., Shizuoka, 3 : 1-77.
Williams, D. F., 1988. Evidence for and against sea-level changes from the stable isotopic record of the Cenozoic. *Soc. Econ. Paleontol. Mineral. Spec. Publ.*, 42 : 31-36.
Woodruff, F., Savin, S. M., and Douglas, R. G., 1981. Miocene stable isotope record : a detailed deep Pacific Ocean study and its paleoclimatic implications. *Science*, 212 : 665-668.

(Manuscript received on June 1, 1992 ; and accepted on June 22, 1992)